

Immunotargeting of Antigen xCT Attenuates Stem-like Cell Behavior and Metastatic Progression in Breast Cancer

Stefania Lanzardo¹, Laura Conti¹, Ronald Rooke², Roberto Ruiu¹, Nathalie Accart³, Elisabetta Bolli¹, Maddalena Arigoni¹, Marco Macagno¹, Giuseppina Barrera⁴, Stefania Pizzimenti⁴, Luigi Aurisicchio⁵, Raffaele Adolfo Calogero¹, and Federica Cavallo¹

Abstract

Resistance to therapy and lack of curative treatments for metastatic breast cancer suggest that current therapies may be missing the subpopulation of chemoresistant and radioresistant cancer stem cells (CSC). The ultimate success of any treatment may well rest on CSC eradication, but specific anti-CSC therapies are still limited. A comparison of the transcriptional profiles of murine Her2⁺ breast tumor TUBO cells and their derived CSC-enriched tumorspheres has identified xCT, the functional subunit of the cystine/glutamate antiporter system x_c⁻, as a surface protein that is upregulated specifically in tumorspheres. We validated this finding by cytofluorimetric analysis and immunofluorescence in TUBO-derived tumorspheres and in a panel of mouse and human

triple negative breast cancer cell-derived tumorspheres. We further show that downregulation of xCT impaired tumorsphere generation and altered CSC intracellular redox balance *in vitro*, suggesting that xCT plays a functional role in CSC biology. DNA vaccination based immunotargeting of xCT in mice challenged with syngeneic tumorsphere-derived cells delayed established subcutaneous tumor growth and strongly impaired pulmonary metastasis formation by generating anti-xCT antibodies able to alter CSC self-renewal and redox balance. Finally, anti-xCT vaccination increased CSC chemosensitivity to doxorubicin *in vivo*, indicating that xCT immunotargeting may be an effective adjuvant to chemotherapy. *Cancer Res*; 76(1); 62–72. ©2015 AACR.

Introduction

Despite recent advances in breast cancer management resulting in a decrease in overall mortality (1), minimal residual disease and local and distant posttreatment recurrences are still major obstacles to complete remission. According to the cancer stem cell (CSC) model, these residual elements are caused by a stem-like subpopulation of tumor cells that are endowed with self-renewal and multilineage differentiation capabilities, chemo- and radio-resistance and the ability to give metastases (2). The therapeutic implication of the CSC model is that a tumor needs to be deprived of its CSC population to be completely eradicated. Novel anticancer strategies must therefore be developed to face this new challenge.

Active immunotherapy, i.e., vaccination, is an attractive approach to target CSC. Preclinical studies have shown that CSC are immunogenic and a more effective antigen source for inducing protective antitumor immunity in mice than unselected tumor cells (3). Several clinical trials in which CSC lysate or mRNA are used to pulse or transfect autologous dendritic cells (DC), that are then injected back into the patients, are currently underway in various tumor settings (4). However, this technique presents the difficulty of setting up standardized functional DC production procedures (5). A promising alternative can be found in powerful and versatile DNA-based vaccines, which combines lower manufacturing costs and more standardized production processes while also inducing strong immunologic responses against tumor antigens. Nevertheless, one must identify a suitable target to develop a DNA-based vaccine; as no consensus on the expression of specific vaccination targets by CSC currently exists, preclinical screening by high-throughput technologies can be of use in uncovering antigens for CSC-targeted genetic vaccines.

We have compared the transcription profile of the murine Her2⁺ breast cancer TUBO cell line (6) with that of its CSC-enriched tumorspheres in order to identify antigens expressed by mammary CSC. Among the genes upregulated in tumorspheres and associated with poor prognosis in several data sets of human mammary cancer, we focused on xCT. It is the light chain of the antiporter system x_c⁻, which imports the amino acid cystine into cells in exchange with glutamate. Cystine is the rate-limiting substrate for the synthesis of the antioxidant glutathione (GSH), which is known to be involved in the detoxification of reactive oxygen species (ROS; ref. 7). xCT is highly expressed by a variety of malignant tumors (7–12) and plays an important role in

¹Department of Molecular Biotechnology and Health Sciences, Molecular Biotechnology Center, University of Turin, Turin, Italy. ²Elsalys Biotech, Illkirch Graffenstaden, France. ³Novartis Institute for Medical Research, Basel, Switzerland. ⁴Department of Clinical and Biological Sciences, University of Turin, Turin, Italy. ⁵Takis, Via di Castel Romano, Rome, Italy.

Note: Supplementary data for this article are available at Cancer Research Online (<http://cancerres.aacrjournals.org/>).

S. Lanzardo and L. Conti contributed equally to this article.

Corresponding Author: Federica Cavallo, University of Turin, Molecular Biotechnology Center, Via Nizza 52, 10126 Turin, Italy. Phone: 39-011-6706457; Fax: 39-011-2365417; E-mail: federica.cavallo@unito.it

doi: 10.1158/0008-5472.CAN-15-1208

©2015 American Association for Cancer Research.

cancer growth, progression, metastatic dissemination (13–15), and drug resistance (16). Moreover, its membrane expression is stabilized via direct interaction with a CD44 variant (CD44v; ref. 13), although targeting xCT has been found to deplete undifferentiated CD44v-expressing cancer cells in a xenografted model of head and neck squamous cell carcinoma, sensitizing the tumor to other therapies (17).

We herein report that xCT upregulation is a general feature of breast CSC and that plays a functional role in CSC biology and intracellular redox balance. We demonstrate that anti-xCT DNA vaccination slows established subcutaneous tumor growth, efficiently impairs lung metastasis formation, and increases CSC chemosensitivity, thus making it a novel therapeutic approach for breast cancer treatment.

Materials and Methods

Cell and tumorsphere cultures

MDA-MB-231, HCC-1806, and 4T1 cells were purchased from the ATCC (LGC Standards) and cultured as in ref. 18. NIH/3T3 cells were cultured as in ref. 19. Cells were passaged in our laboratory for fewer than 6 months after their resuscitation. TUBO cells and tumorspheres were generated as in ref. 18. Human cell lines were tested utilizing short tandem repeat profiling.

FACS analysis

Cells and tumorspheres were stained with AlexaFluor647-anti-Sca-1, PE-anti-CD44, and PE/Cy7-anti-CD24 (Biolegend), and with goat anti-xCT (Santa Cruz Biotechnology) antibodies followed by rabbit FITC-anti-goat Ig (Dako), or with Aldefluor kit (StemCell Technologies), as in ref. 18. To quantify anti-xCT antibody titers, tumorsphere-derived and NIH/3T3 cells were incubated with sera of vaccinated mice and subsequently with rabbit FITC-anti-mouse Ig (Dako). Cells were stained with 2',7'-dihydrochlorofluorescein diacetate (DHCF-DA, Sigma-Aldrich) as in ref. 20. All samples were analyzed on a CyAnADP Flow Cytometer, using the Summit 4.3 software (Beckman Coulter).

Fluorescent microscopy

Tumor microarrays (TMA; Biochain # T8234700-2, lot # B406087, and Biochain # T6235086-5, lot # B112136) of normal or tumor human tissues were blocked in 3% H₂O₂ (Sigma-Aldrich), followed by 1% BSA, and then incubated with anti-xCT or isotype-matched control antibodies (Abcam). The signal was amplified as in ref. 21 and sections were fixed in 1% formaldehyde (Sigma-Aldrich), counterstained with DAPI (Sigma-Aldrich), and mounted in Mowiol (Calbiochem). Images were acquired using a confocal microscope LSM700 and Zen software 7.0.0.285 (Zeiss). Slides were scanned on a slide scanner (Hamamatsu Nanoscope 2.0RS) using the Calopix software. xCT⁺ cell percentage was defined by quantifying blue (nuclei) and red (xCT) surface areas and calculated as the ratio of xCT expression (i.e., xCT stained surface/xCT + nuclei surface).

Tumorspheres were cytospinned to glass slides, fixed in 4% formaldehyde and then incubated with rabbit anti-OCT4 (Abcam), rat PE-anti-Sca-1 (Santa Cruz Biotechnology), mouse APC/eFluor780-anti-Thy1.1 (eBioscience), or the matched isotype control antibodies. Cytospinned tumorspheres or NIH/3T3 cultured on glass coverslips were stained with IgG purified from immunized mice sera and then with rabbit AlexaFluor488-anti-mouse or goat Texas red-anti-rabbit secondary antibodies (Life

Technologies). Images were acquired on the ApoTome system and AxioVision Release4.8 software (Zeiss).

In vitro cytotoxicity

Twenty-four hours after TUBO cells and tumorspheres seeding in 96-well plates, scalar doses of doxorubicin or sulfasalazine (SASP; Sigma-Aldrich) were added and incubated at 37°C for 72 hours. Cytotoxicity was evaluated with MTT using the Cell Proliferation Kit I (Roche Diagnostics).

RNA interference

xCT downregulation in tumorspheres was performed using a pool of specific siRNAs, or scrambled siRNAs (Invitrogen Corp.), as in ref. 18.

SASP effects on tumorsphere formation

Dissociated tumorspheres were cultured with scalar doses of SASP or its diluent DMSO (Sigma-Aldrich), and the total number of tumorspheres/well was counted 5 days later.

Measurement of ROS and GSH

ROS amount was analyzed as 2',7'-dichlorofluorescein (DCF) formation in cells incubated with 5 μmol/L DHCF-DA for 20 minutes at 37°C using the Luminescence Spectrometer LS 55 (Perkin-Elmer), quantified using a DCF standard curve, and expressed as pmol DCF formed/min/mg protein (22). GSH content was assessed by determining nonprotein sulphhydryl content, as in ref. 23, and calculated using a GSH standard curve. Results are expressed as μg GSH/mg of cellular proteins.

Plasmids

The cDNA sequence for mouse xCT (NM_011990.2), in the pDream2.1 plasmid (GenScript), was cloned in a pVAX1 (Invitrogen) plasmid (pVAX1-xCT), sequenced (BMR Genomics), and produced with EndoFree Plasmid Giga Kits (Qiagen Inc.).

Immune sera effect on tumorsphere formation

Serum IgG from vaccinated mice were purified using the Melon Gel Purification Kit (Thermo Scientific) and incubated with tumorsphere-derived cells. After 5 days, spheres were counted and analyzed for CSC markers expression and ROS production by FACS.

In vivo treatments

Female 6- to 8-week-old wild-type (Charles River Laboratories) and Ig μ-chain gene knocked out (BALB-μIgKO; ref. 24) BALB/c mice were maintained at the Molecular Biotechnology Center, University of Turin, and treated in accordance with the University Ethical Committee and European guidelines under Directive 2010/63. Vaccination, performed either before or after tumor challenge, consisted of two intramuscular electroporations at 2 weeks interval, of pVAX1 or pVAX1-xCT plasmids as previously described (25).

Primary s.c. tumors were induced by injecting 1×10^4 TUBO or 4T1 tumorsphere-derived cells. Some tumors were explanted and tumorspheres generated as in ref. 26. Lung metastases were induced either by injecting i.v. 5×10^4 TUBO tumorsphere-derived cells or by injecting s.c. 1×10^4 4T1 tumorsphere-derived cells. In the latter case, lungs were removed when s.c. tumors reached 10 mm mean diameter. Micrometastases were counted on a Nikon SMZ1000 stereomicroscope (Mager Scientific).

Doxorubicin treatment consisted of the i.v. administration of a total dose of 10 mg/Kg either in a single injection or in two administrations at a week interval.

Statistical analysis

Differences in latency, sphere formation, protein expression, GSH, and ROS levels and metastasis number were evaluated using a Student *t* test. Data are shown as the mean \pm SEM unless otherwise stated. Values of $P < 0.05$ were considered statistically significant.

Results

xCT is upregulated in breast CSC

To identify the transcripts associated with mouse and human mammary CSC, we compared the transcription profile of Her2⁺ murine TUBO cells, which had been cultured as an epithelial monolayer, with the profiles of the first three *in vitro* passages of their derived tumorspheres (P1, P2, and P3) using MouseWG-6 v2.0 Illumina beadchips (GSE21451; Supplementary Fig. S1A). This analysis uncovered a cluster of transcripts whose expression rose, as well as three clusters whose expression decreased from TUBO through P1 to P3 cells (Supplementary Fig. S1B).

We devised a ranking procedure according to the clinical outcome of tumors expressing the transcripts that we found increased in tumorspheres (27), using data from six public human breast cancer data sets (see Supplementary Methods). One of the genes with the best clinical outcome score was xCT (*Slc7a11*, Supplementary Fig. S1C; ref. 7), whose expression increased progressively from TUBO to P3 tumorspheres, as confirmed by FACS (Fig. 1A) and qPCR (Supplementary Fig. S2) analyses. Interestingly, most P3-derived cells that express the stem cell marker Sca-1 (26) are also xCT⁺ (Fig. 1B). The immunofluorescence analysis revealed widespread xCT positivity in tumorspheres that are essentially composed of CSC, as confirmed by Sca-1, OCT4, and Thy1.1 marker expression patterns (Fig. 1C). xCT upregulation is a feature of breast CSC and is not due to tumorsphere culture conditions, because it was also observed on the small CD44^{high}/CD24^{low} CSC population present in TUBO cells (Fig. 1D). Moreover, xCT upregulation is not restricted to TUBO-derived CSC as it was also observed in tumorspheres derived from mouse (4T1) and human (HCC-1806 and MDA-MB-231) triple negative breast cancer (TNBC) cell lines (Fig. 1E), suggesting that xCT may be a hallmark of breast cancer CSC.

xCT expression in the TMA of normal and neoplastic samples was evaluated to address its distribution in human cancers. xCT expression was low in normal mammary glands (Fig. 1F, left) as it was in the other normal tissues tested (Supplementary Fig. S3A). By contrast, xCT was expressed at high levels in many neoplastic tissues (Supplementary Fig. S3B), including hyperplastic mammary lesions and invasive ductal breast carcinomas (IDC; Fig. 1F, middle and right) displaying a pattern in which it is confined to neoplastic cells. In particular, we found xCT expression in 62% of Her2⁺, 57% of estrogen/progesterone receptor⁺ Her2⁻ (ER/PR⁺Her2⁻), and 35% of TNBC samples (Fig. 1G), suggesting that xCT may well be a commonly upregulated target in breast cancers.

xCT downregulation impairs tumorsphere generation and alters intracellular redox balance

A MTT test was performed on TUBO cells and tumorspheres that had either been treated or not with scalar doses of xCT inhibitor SASP (28). Although SASP did not decrease TUBO

cell viability, except for the highest dose (100 μ mol/L; IC₅₀, 126.1 \pm 25.7 μ mol/L; Fig. 2A), tumorsphere viability was inhibited in a dose-dependent manner (IC₅₀, 51.6 \pm 3.5 μ mol/L; Fig. 2B), suggesting that CSC are sensitive to xCT inhibition. Similarly, xCT silencing through a pool of specific siRNAs impaired tumorspheres but not TUBO cell viability (Fig. 2A and B). Moreover, SASP treatment and xCT silencing impaired tumorsphere generation (Fig. 2C and D). FACS analyses performed 24 hours after siRNA transfection showed that the reduction in xCT⁺ cells (Fig. 2E and F) is accompanied by a reduction in CSC, i.e., Sca1⁺ and CD44^{high}/CD24^{low} cells (Fig. 2F). On the contrary, xCT overexpression increases colony generating ability, as confirmed by the higher number of colonies generated in soft agar by NIH/3T3 and HEK-293 cells transfected with xCT when compared with the corresponding cells transfected with empty plasmids (Supplementary Fig. S4). Taken together, these data suggest that xCT plays an important role in CSC maintenance and sphere generation.

As xCT is an important determinant of redox balance (13), we evaluated GSH and ROS levels in TUBO cells and tumorspheres. GSH amount was significantly greater in tumorspheres than in TUBO cells (Fig. 2G), whereas ROS levels were lower (Fig. 2H). xCT downregulation caused a significant decrease in GSH and an increase in ROS levels (Fig. 2G and H) as compared with controls, suggesting that CSC have a higher ROS defense capability than epithelial tumor cells.

Anti-xCT vaccination induces antibodies that inhibit CSC

BALB/c mice were vaccinated with either pVAX1-xCT or pVAX1 to evaluate whether xCT is a potential target for cancer immunotherapy. No T-cell response was observed against the H-2K^d dominant mouse xCT peptide (Supplementary Fig. S5A and S5B). Tumorsphere-derived cells were stained with the sera of vaccinated mice to evaluate their humoral response, and specific antibody binding was analyzed by FACS. pVAX1-xCT vaccination induced the production of CSC-binding antibodies, which were not detectable in empty pVAX1-vaccinated mouse sera (Fig. 3A–C). These results were confirmed by the ability of purified IgG, from pVAX1-xCT-vaccinated mouse sera, to stain tumorspheres (Fig. 3D). These antibodies are specific for xCT, as no binding was observed in NIH/3T3 cells negative for xCT expression (Fig. 3E–H).

Of note, TUBO cells incubated with IgG purified from pVAX1-xCT-vaccinated mice displayed reduced sphere-generation ability (Fig. 3I), a lower percentage of stem cell marker positive cells (Fig. 3J), but increased ROS content as compared with control IgG (Fig. 3K).

These results suggest that anti-xCT vaccination induces antibodies targeting xCT, thus affecting self-renewal and ROS production in CSC.

Anti-xCT vaccination slows *in vivo* breast tumor growth

TUBO-derived tumorspheres were s.c. implanted into BALB/c mice that were vaccinated when tumors reached 2 or 4 mm mean diameter to evaluate whether xCT immune-targeting hinders breast cancer growth (Fig. 4A–D). Tumors grew progressively in the pVAX1 group of 2 mm vaccinated mice (Fig. 4A), although tumors regressed in 23.8% of pVAX1-xCT-vaccinated mice (Fig. 4B). Tumor growth kinetics were slower in the latter group than in the pVAX1 group, as proven

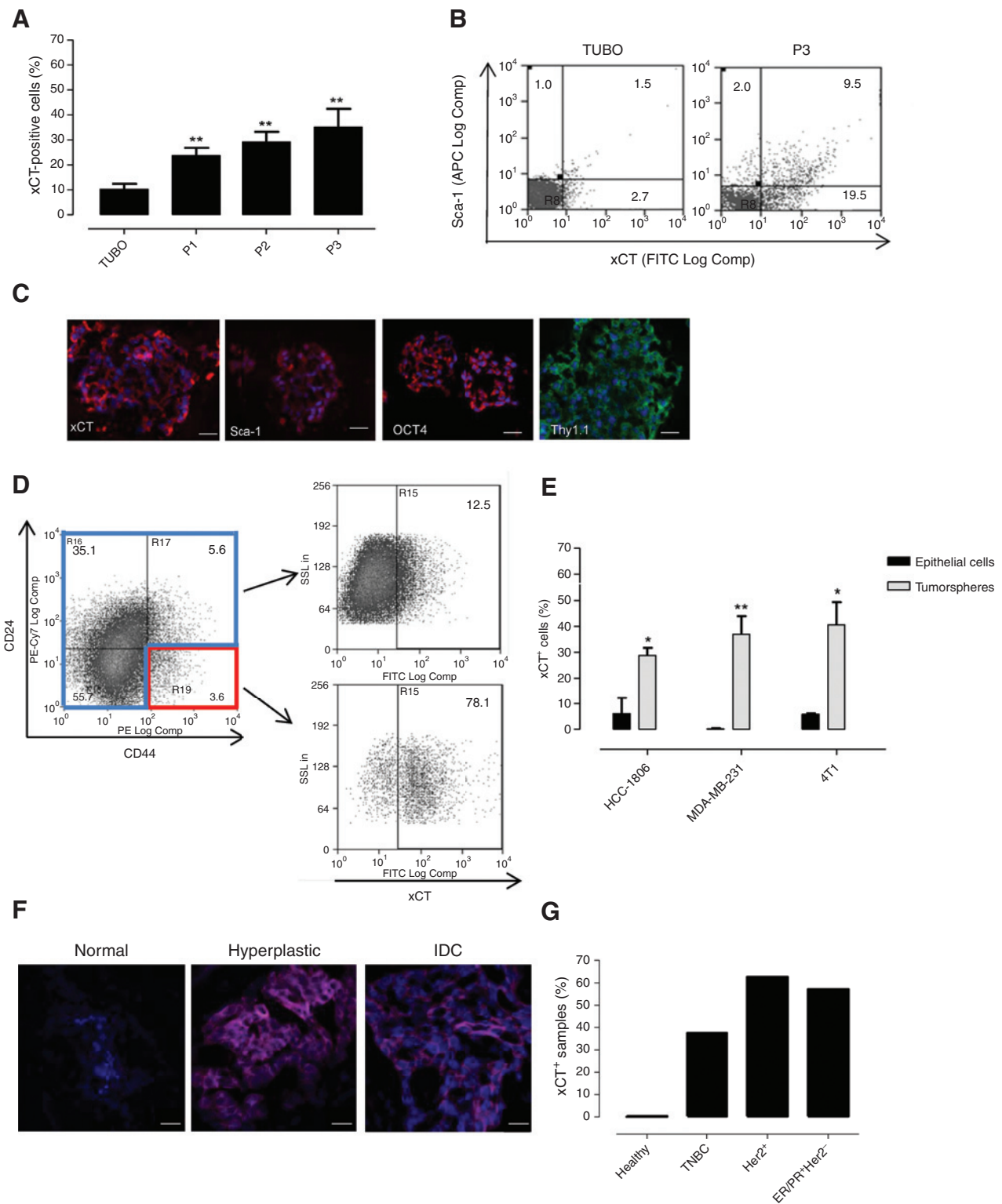


Figure 1. xCT expression in breast CSC and tumors. A, FACS analysis of xCT expression in TUBO cells and P1 to P3 tumorsphere passages over six independent experiments. B, representative density plots of xCT and Sca-1 expression on TUBO and tumorspheres. Numbers show the percentage of cells in each quadrant. C, representative immunofluorescence staining of xCT, Sca-1, OCT4, and Thy1.1 on tumorspheres. DAPI stains the nucleus. Scale bar, 20 μm. D, representative density plots of xCT expression in TUBO cells stained with CD44 and CD24. E, FACS analysis of xCT expression in HCC-1806, MDA-MB-231, and 4T1 cells and their derived tumorspheres over three independent experiments. *, $P < 0.05$; **, $P < 0.01$; ***, $P < 0.001$, Student t test. F, immunofluorescence of xCT expression (red) in normal breast, hyperplastic, and IDC breast carcinoma. Scale bar, 20 μm. G, percentage of xCT+ samples in normal mammary gland and in TNBC, Her2+, or ER/PR+Her2- breast cancer subtypes.

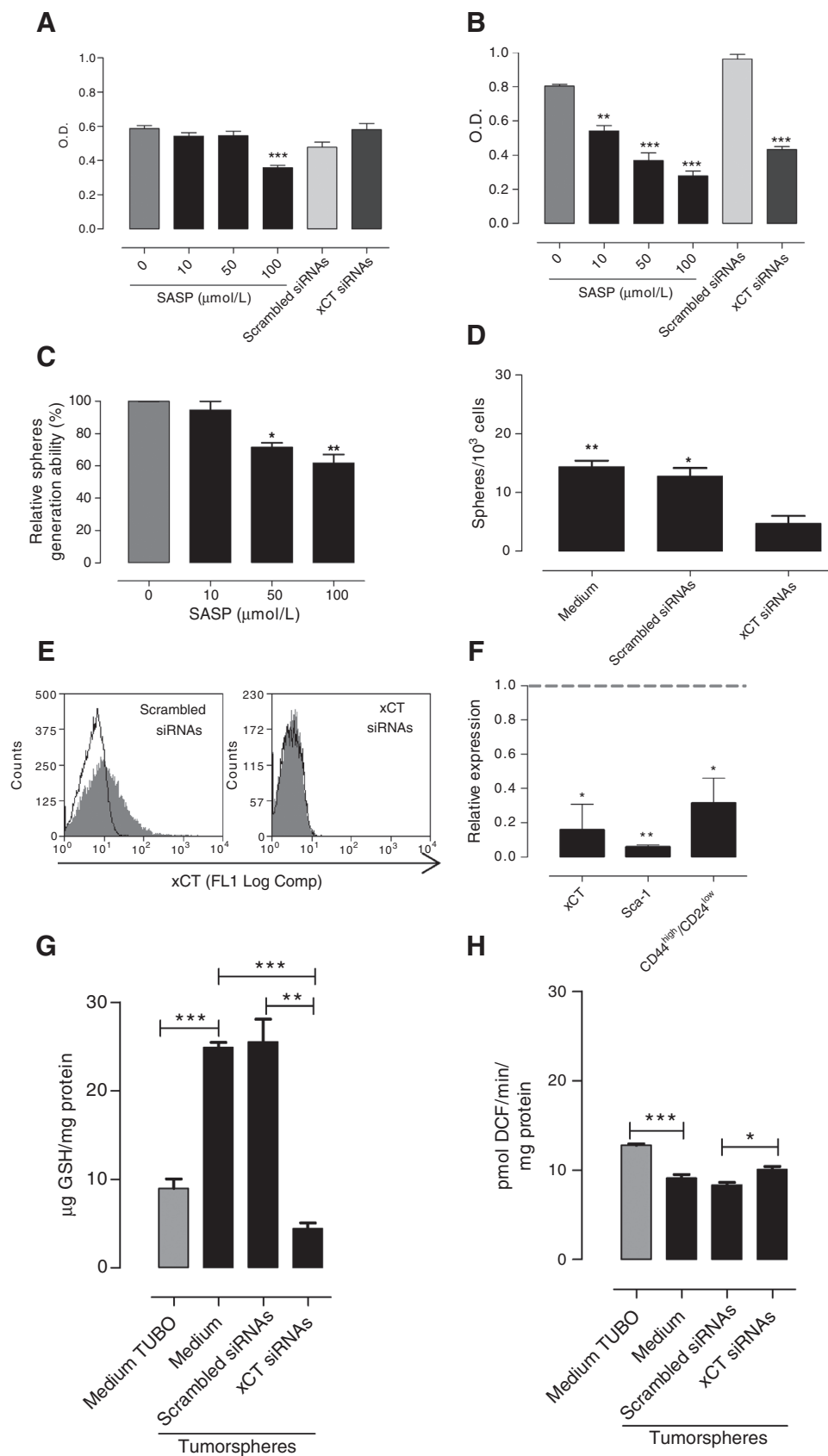
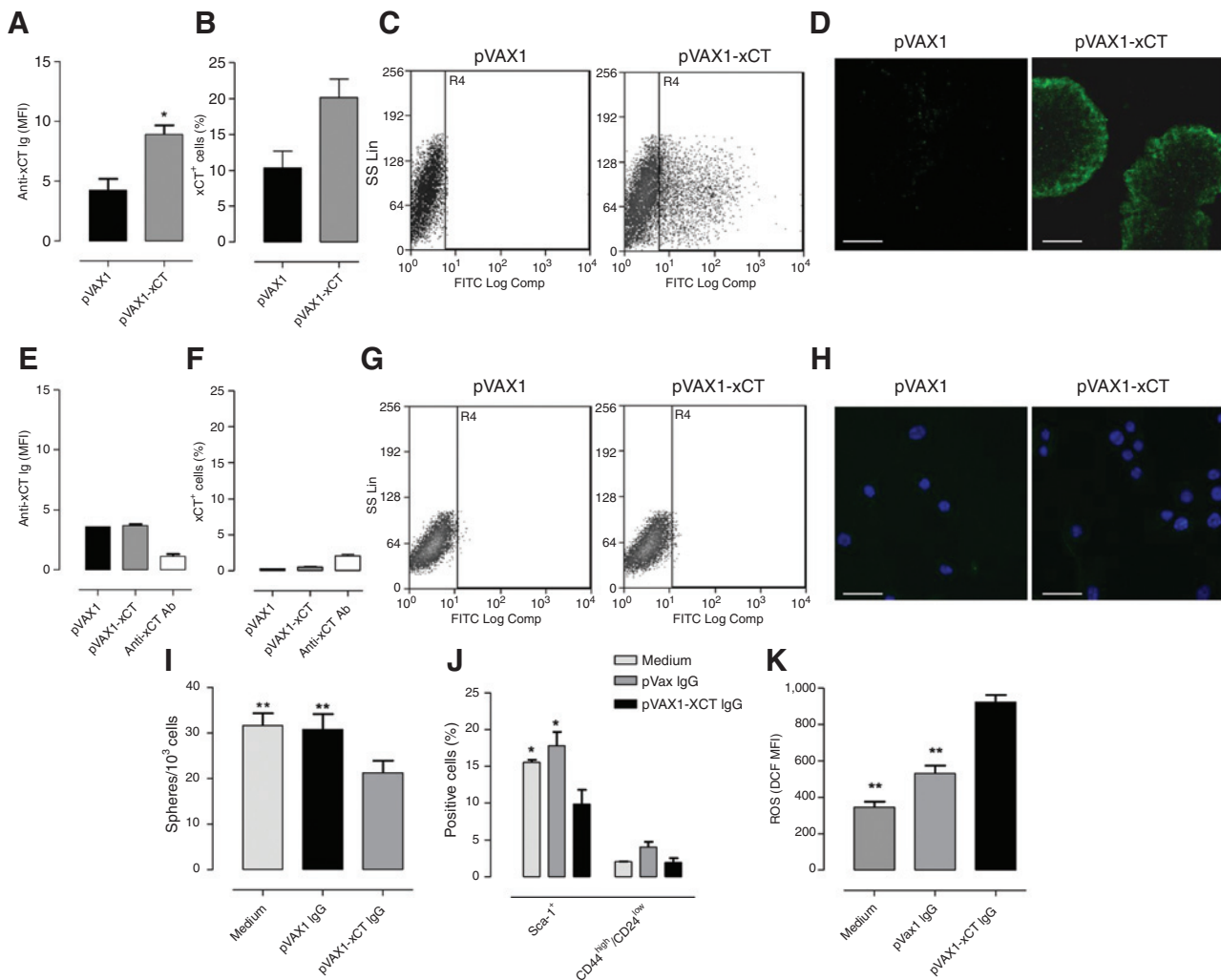


Figure 2. xCT regulates CSC self-renewal and the intracellular redox balance. A and B, MTT assay of the cytotoxic effect exerted by scalar doses of SASP or by anti-xCT siRNAs on TUBO (A) and tumorspheres (B). C, sphere generation ability relative to untreated cells of tumorspheres incubated with SASP. D, sphere generation ability of tumorspheres incubated with siRNAs to xCT, scrambled siRNAs, or not at all shown as tumorsphere number/10³ plated cells. E and F, FACS analysis of xCT and CSC marker expression in spheres 24 hours after transfection with siRNAs to xCT or scrambled siRNAs. E, gray histograms show xCT expression; open histograms show the background of negative control IgG stained cells from one representative experiment. F, relative expression (%) of xCT⁺, Sca-1⁺, and CD44^{high}/CD24^{low} cells in tumorsphere-derived cells transfected with siRNAs to xCT (black bars) compared with cells transfected with scrambled siRNAs (dashed line). G and H, GSH (G) and ROS (H) levels in TUBO cells and their derived tumorspheres after either seeding in normal conditions, transfection with siRNAs to xCT, or scrambled siRNAs over three independent experiments. *, *P* < 0.05; **, *P* < 0.01; ***, *P* < 0.001, Student *t* test.

Downloaded from <http://aacrjournals.org/cancerres/article-pdf/76/1/62/2732081/62.pdf> by guest on 29 April 2025

**Figure 3.**

Vaccine-induced antibodies target CSC and affect their self-renewal and ROS flux. A–G, TUBO-derived tumorsphere (A–C) or NIH/3T3 cell staining by antibodies present in the sera of BALB/c mice vaccinated with pVAX1 or pVAX1-xCT (E–G), analyzed by FACS. Results are reported as the mean fluorescence intensity (MFI; A and E) from 7 mice per group, the percentage of positive cells (B and F), and two representative dot plots (C and G). D and H, representative images of TUBO-tumorspheres (D) or NIH/3T3 cells stained with IgG purified from sera of mice vaccinated with pVAX1 or pVAX1-xCT (H). Scale bar, 20 μ m. I, sphere generating ability of tumorspheres incubated for 5 days with IgG purified from the sera of mice vaccinated with pVAX1, pVAX1-xCT, or not at all. Graph shows tumorsphere number/10³ plated cells. FACS analysis of CSC marker expression (J) or ROS production (K) in tumorspheres incubated for 5 days with IgG purified from the sera of vaccinated mice or not at all, reported as percentage of positive cells (D) or DCF MFI (E) from four independent experiments. *, $P < 0.05$; **, $P < 0.01$, Student t test.

by the significantly shorter time required for tumors to reach 4 or 6 mm mean diameter (20.7 ± 2.7 and 30.7 ± 3.6 days in pVAX1-xCT-vaccinated mice vs. 12.9 ± 2 and 20.8 ± 2.5 days in control mice). Anti-xCT vaccination also induced tumor regression in 16% of mice that were treated when their tumors measured 4 mm mean diameter (Fig. 4D), while all tumors in the pVAX1 group reached 10 mm mean diameter in less than 60 days (Fig. 4C). The efficacy of anti-xCT vaccination was then evaluated against 2 or 4 mm mean diameter tumors obtained when 4T1 tumorsphere-derived cells were injected s.c. (Fig. 4E–H). In 2 mm tumor-vaccinated mice, tumors grew rapidly in pVAX1 group (Fig. 4E), while tumor growth kinetics were generally slower and the time required for the tumors to reach 4, 6, 8, or 10 mm mean diameter was significantly longer

in the pVAX1-xCT-vaccinated group (10.4 ± 1.3 ; 15.6 ± 1.6 ; 20.4 ± 1.3 ; 23.4 ± 1.2 days in pVAX1-xCT-vaccinated mice vs. 4.9 ± 0.5 ; 10 ± 1.1 ; 14.6 ± 1.0 ; 17.4 ± 0.8 days in control mice). Similarly, the 4 mm tumor-vaccinated group displayed slower tumor growth in pVAX1-xCT-vaccinated mice (Fig. 4E and H), and the time required for the tumors to reach 6, 8, or 10 mm mean diameter was significantly longer (9.2 ± 0.9 ; 13.1 ± 0.9 ; 17.0 ± 0.5 days in pVAX1-xCT-vaccinated mice vs. 5.2 ± 0.9 ; 8.8 ± 1.0 ; 13.0 ± 1.6 days in control mice), indicating that xCT immunotherapy may be beneficial in various breast cancer subtypes.

Tumor remission in vaccinated mice might be due to a reduction of CSC frequency as a consequence of the treatment, as suggested by the decrease in the percentage of Aldefluor⁺ cells

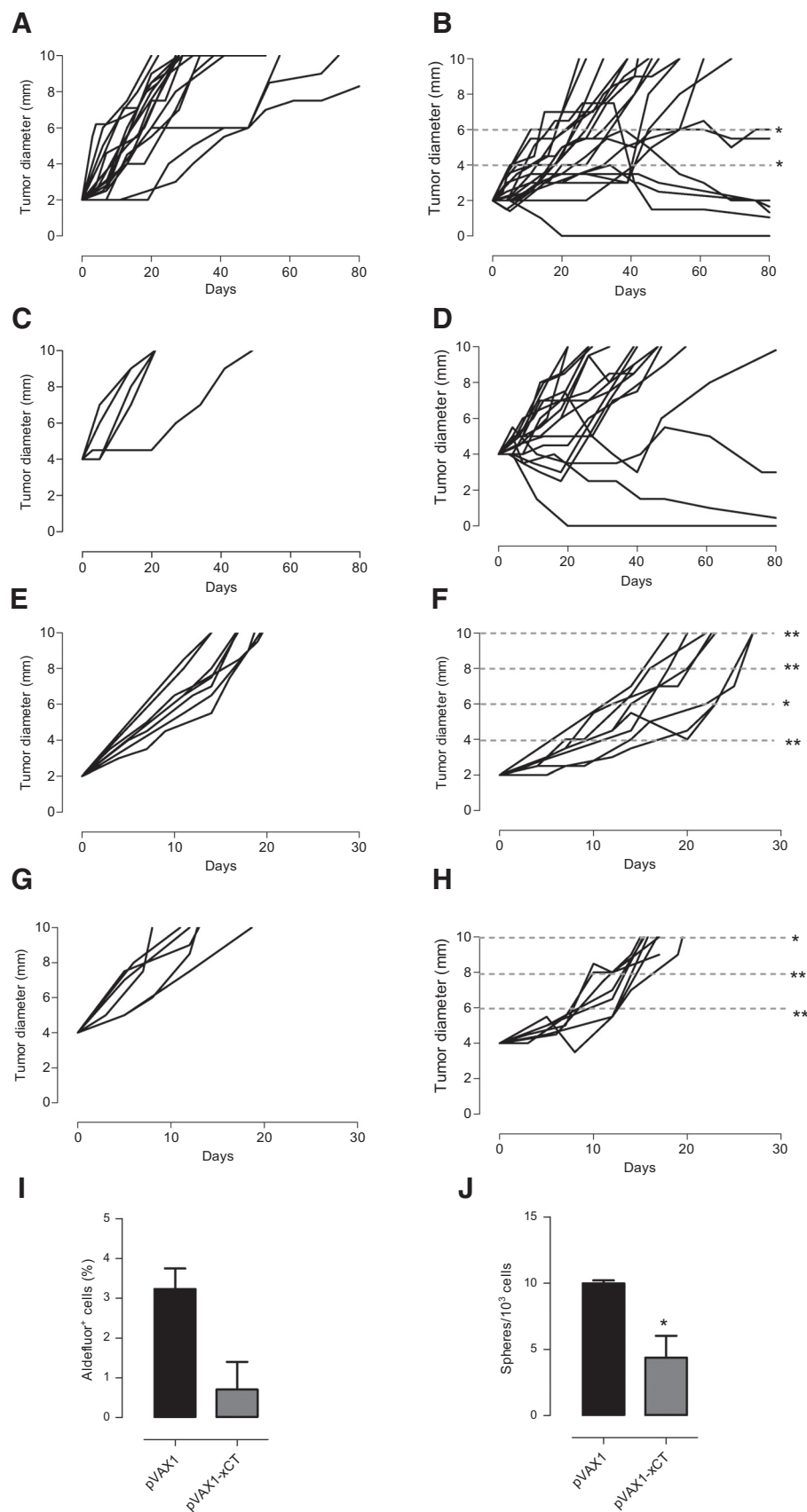


Figure 4. Anti-xCT vaccination delays CSC-induced tumor growth *in vivo*. BALB/c mice were s.c. challenged with tumorspheres derived from either TUBO (A-D) or 4T1 (E-H) cells and electroporated with pVAX1 (A, C, E, and G) or pVAX1-xCT (B, D, F, and H) plasmids when their tumor reached 2 (A, B, E, and F) or 4 mm (C, D, G, and H) mean diameter. Each black line depicts the growth of a single tumor. Data were cumulated from three independent and concordant experiments. Statistically significant differences in mean time required for pVAX1-xCT group and pVAX1 group tumors to reach 4, 6, 8, or 10 mm mean diameter are indicated by dashed gray lines. I and J, analysis of the percentage of Aldefluor⁺ cells in tumors explanted from vaccinated mice challenged s.c. with TUBO-derived tumorspheres (I) and the number of tumorspheres generated *in vitro* by cells from the same tumors (J). *, $P < 0.05$; **, $P < 0.01$, Student *t* test.

Downloaded from <http://aacrjournals.org/cancerres/article-pdf/76/1/62/2732081/62.pdf> by guest on 29 April 2025

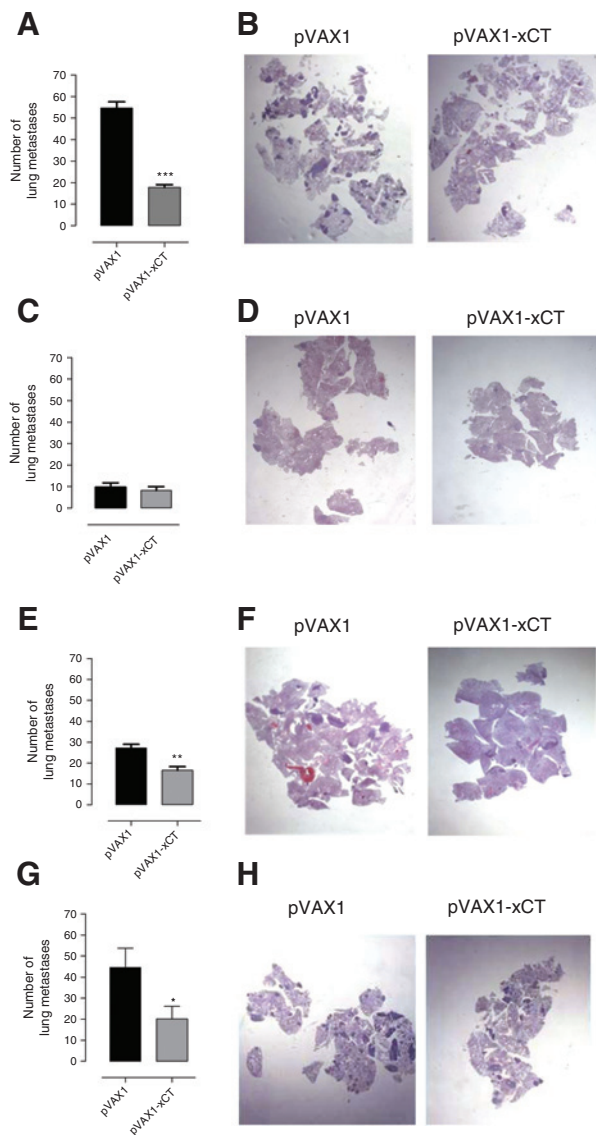


Figure 5. Anti-xCT vaccination reduces CSC-generated lung metastasis formation. BALB/c (A, B, E, and H) and BALB- μ IgKO (C and D) mice were vaccinated with either pVAX1 or pVAX1-xCT plasmids before tumorspheres injection (A, C, and E) or when mice had 2 mm mean diameter tumor (G). Number of lung metastases in mice challenged i.v. with TUBO- (A and C) or s.c. with 4T1-derived tumorspheres (E and G) and enumerated 20 days later (A and C) or when the primary tumor reached 10 mm mean diameter (E and G). B, D, F, and H, representative images of lung metastases after H&E staining. **, $P < 0.01$; ***, $P < 0.001$, Student t test.

in regressing tumors from mice vaccinated with pVAX1-xCT plasmid (Fig. 4I). Moreover, the cells composing the tumor mass had a significantly decreased tumorsphere forming ability (Fig. 4J) when compared with cells derived from tumors grown in pVAX1-vaccinated mice.

Anti-xCT vaccination prevents lung metastasis formation

BALB/c mice were vaccinated with pVAX1 or pVAX1-xCT plasmids and i.v. injected with TUBO-derived tumorspheres

to evaluate the effects of anti-xCT vaccination on lung metastasis formation. Metastasis number was significantly reduced after pVAX1-xCT vaccination, as reported in Fig. 5A and B. This antimetastatic effect is dependent on the specific antibodies elicited by anti-xCT vaccination, because no effect was observed vaccinating BALB- μ IgKO mice i.v. injected with TUBO-derived tumorspheres (Fig. 5C and D).

Anti-xCT vaccination was also able to reduce the number of spontaneous metastases generated from the s.c. injection of 4T1-derived tumorspheres, either when vaccination was performed before tumorsphere injection (Fig. 5E and F) or when mice already had a 2-mm mean diameter tumor (Fig. 5G and H).

Altogether, these findings suggest that anti-xCT vaccination interferes with CSC metastatic properties both in a preventive and therapeutic setting. This antimetastatic activity is due to CSC immunotargeting, because no effect was observed in xCT-vaccinated mice injected with differentiated tumor cells (Supplementary Fig. S6A and S6B) or in mice vaccinated against Her3 (29) and injected with TUBO-derived tumorspheres (Supplementary Fig. S7A–S7F). In this model Her3 is not a CSC-specific antigen, because it is equally expressed on TUBO cells and tumorspheres.

Anti-xCT vaccination enhances the effect of doxorubicin

In accordance with CSC resistance to chemotherapy (2), TUBO cells display a higher sensitivity to doxorubicin than tumorspheres (Fig. 6A and B). Because xCT is involved in maintaining the intracellular redox balance, thus counteracting the effects of ROS-generating cytotoxic drugs (13), it is likely that targeting xCT could increase CSC chemosensitivity. In order to explore this hypothesis *in vivo*, unvaccinated, pVAX1-xCT, and pVAX1-vaccinated mice were i.v. injected with TUBO-derived tumorspheres and either treated with doxorubicin or not. As shown in Fig. 6C, pVAX1-xCT determined a decrease in the number of lung metastases compared with the control and doxorubicin-treated mice and the combination of vaccination and doxorubicin significantly improved the activity of individual treatments.

Similar results were observed in mice challenged with s.c. injection of TUBO-derived tumorspheres and subjected to vaccination and chemotherapy when tumors reached 2 mm mean diameter. The tumor regressed in 25% of mice treated with doxorubicin alone (Fig. 6D) or in combination with pVAX1 plasmid (Fig. 6E), although the combination of doxorubicin and anti-xCT vaccination stopped tumor progression in 60% of mice (Fig. 6F).

All together, these data suggest that anti-xCT vaccination may well be an efficient adjuvant treatment for chemotherapy both in a preventive and in a therapeutic setting.

Discussion

A key challenge in anticancer therapy is the development of treatments able to both shrink a tumor and kill CSC, which are resistant to current chemo- and radiotherapies, and are considered the source of tumor recurrence and metastatic spread. However, the identification of ideal CSC-associated targets is a particularly tough task because CSC appear to be "moving targets" that switch between different cell states during cancer progression (30). Hence, antigens that are upregulated in CSC but also present in

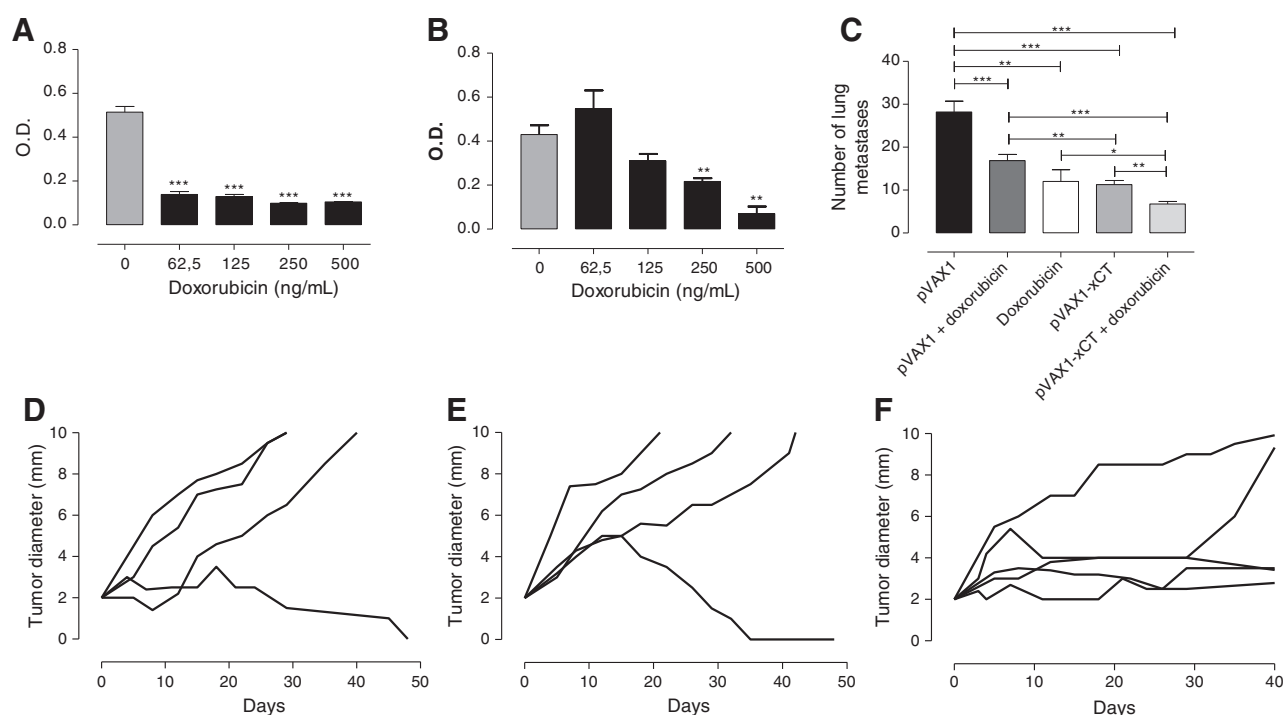


Figure 6.

Anti-xCT vaccination enhances the effect of doxorubicin *in vivo*. A and B, MTT assay of the cytotoxic effect exerted by incubation with scalar doses of doxorubicin in TUBO (A) and tumorspheres (B). C, number of lung metastases in mice challenged i.v. with TUBO-derived tumorspheres and either vaccinated or not with pVAX1 and pVAX1-xCT plasmids alone or in combination with doxorubicin administration. D-F, tumor growth curves of BALB/c mice s.c. injected with TUBO-derived tumorspheres and treated with doxorubicin in combination with pVAX1 (E) or pVAX1-xCT (F) vaccination when their tumors reached 2 mm mean diameter. Treatments were repeated the week later. Each black line depicts the growth of a single tumor. *, $P < 0.05$; **, $P < 0.01$; ***, $P < 0.001$, Student *t* test.

more differentiated cancer cells would appear to be outstanding candidates.

A possible candidate with these features is xCT, which we have identified as upregulated in breast Her2⁺ and TNBC CSC. Importantly, its expression is not confined to CSC, because we were able to detect its presence on cancer cells in human hyperplastic mammary glands as well as in IDC, independently from their histologic subtype. xCT possesses all the features of an ideal target for immunotherapy against undifferentiated and more differentiated cancer cells. This speculation is strengthened by our meta-analyses, performed on human breast cancer data sets, which link high xCT expression to poor prognosis.

Moreover, xCT expression is not limited to breast cancer. Our analyses, performed on a plethora of healthy and neoplastic tissues, and data obtained elsewhere in other tumors (7, 31, 32) have identified xCT as a distinctive cancer marker and suggested that its targeting may be of benefit in the treatment of a wide range of neoplastic diseases.

Another important feature of xCT as immunotherapy target is its functional role, which becomes essential in CSC. Indeed, the impairment of sphere generation following the pharmacologic or genetic downregulation of xCT reflects the role of this protein in the regulation of CSC self-renewal, indicating that xCT is not a simple bystander of the stem-like phenotype in breast cancer, but that it also plays a role in CSC biology.

xCT function in CSC self-renewal might be mediated by the regulation of the mechanisms that govern CSC intracellular redox

balance. Although further studies are needed to better define this mechanism in our model, it has been shown that intracellular ROS concentration can affect CSC viability and self-renewal (33–35). CSC upregulate the key regulator of the antioxidant response nuclear factor erythroid 2-related factor 2 (36) and many antioxidant enzymes, such as superoxide dismutase 2, GSH peroxidases, and heme oxygenase 1, which attempt to maintain intracellular ROS at levels lower than those observed in differentiated cancer cells (37). In accordance with this, a basal increase in GSH and decrease in ROS levels were observed in tumorspheres as compared with TUBO cells, which can be explained by xCT upregulation in tumorspheres and proven by the fact that xCT downregulation reverts this phenotype.

Several authors have advocated the use of xCT as a therapeutic target for pharmacologic inhibition using the administration of SASP, a FDA-approved, anti-inflammatory drug for the treatment of inflammatory bowel disease, ulcerative colitis, and Crohn's disease (38). However, SASP exerts many effects in addition to its ability to interfere with xCT function, so it cannot be considered a specific xCT inhibitor (39). Although recent preclinical models demonstrated that SASP impairs cancer growth and metastatic spread via xCT inhibition (15, 17, 40), its use in cancer patients is hampered by its low specificity, short bio-availability, and numerous side effects (41).

We have chosen DNA-based antitumor vaccination as our xCT targeting option on the basis of our consolidated expertise in the field and the considerations stated above. In fact, DNA

vaccination is a cost-effective technology able to induce a significant immune activation against tumor antigens in a specific and well tolerated way, thus reducing off-target effects (42). This paper sees the first report of xCT being targeted with a DNA-based vaccination strategy that efficiently slows mammary tumor growth and prevents lung metastasis formation. Our data show that, despite xCT being a self-antigen, DNA vaccination is able to induce an antibody-based immune response against the tumor; a lack of T-cell response against xCT may be caused by a thymic depletion of high-avidity T-cell clones, as we have previously reported for the Her2 antigen in the BALB-neuT model (43). Notably, the antitumor effects were lost in B cell-deficient mice, confirming the central role of vaccine-induced antibodies. The antitumor effects observed *in vivo* may result from the CSC self-renewal and redox balance impairment induced by anti-xCT antibodies, as indicated by our *in vitro* observations. This is particularly evident in the inhibition of lung metastasis formation, most likely because CSC self-renewal is essential for re-initiating growth at the metastatic site (44).

Interestingly, we were not able to detect any vaccine side effect as xCT expression in normal tissues is almost completely limited to the brain, which can barely be reached by circulating antibodies by virtue of the blood-brain barrier (45). However, it has been reported that xCT may also regulate immune cell functions. In fact, xCT mediates cystine uptake in macrophages and DC, which are the only source of free cysteine release, which, in turn, is essential for the antigen-driven activation of T lymphocytes (46). However, by vaccinating mice against both xCT and Her2, we observed that xCT targeting does not impair the Her2-specific T-cell response (Supplementary Fig. S5C and S5D). The safety of xCT immune targeting is further sustained by the fact that its genetic ablation in mice does not alter vital biologic functions (47).

xCT participate in cancer cells' resistance to a variety of anti-tumor drugs (16). Its action here is thought to be linked to its role in intracellular redox balance, as many chemotherapeutic drugs exert their function, at least in part, by increasing oxidative stress (48). It is worth noting that tumorspheres display significantly increased resistance to doxorubicin, a drug largely used in breast cancer therapy, as compared with epithelial TUBO cells. This fits with the observation that CSC are chemo-resistant (2), and may reflect the increased expression of xCT in tumorspheres. In this regard, it has been demonstrated that xCT inhibition promotes the sensitization of tumor cells to doxorubicin (49, 50). In accordance with these findings, we have observed that a combination of anti-xCT vaccination and doxorubicin strongly enhanced the antimetastatic potential of the individual treatments. This observation strengthens the translatability of this immunotherapeutic approach to clinical trials, where new exper-

imental protocols are routinely tested in combination with standard treatments.

In conclusion, we have shown for the first time that xCT immunotargeting is effective in impairing tumor growth and metastasis formation *in vivo*. We propose a mechanism by which anti-xCT vaccination exerts its antineoplastic function across two separate, but complementary, fronts: (i) a direct effect on CSC through immune-mediated eradication and (ii) inhibition of xCT function on CSC, leading to impairment of tumorigenic and stem-like properties and their sensitizing to chemotherapy. Moreover, a possible additional anticancer mechanism may occur, by which the anti-xCT antibodies induced by vaccination may suppress the myeloid-derived suppressor cells that exploit xCT for their inhibitory activity (46). However, this hypothesis is still to be verified.

Further studies will thoroughly investigate the interactions between chemotherapy and anti-xCT vaccination and all possible side effects in order to accelerate translation to the clinic, as a safe tool to combat CSC in patients is sorely needed.

Disclosure of Potential Conflicts of Interest

No potential conflicts of interest were disclosed.

Authors' Contributions

Conception and design: S. Lanzardo, L. Conti, R. Rooke, F. Cavallo
Development of methodology: S. Lanzardo, L. Conti, R. Ruiu, N. Accart, E. Bolli, M. Arigoni, M. Macagno, F. Cavallo
Acquisition of data (provided animals, acquired and managed patients, provided facilities, etc.): S. Lanzardo, L. Conti, R. Rooke, R. Ruiu, N. Accart, E. Bolli, M. Arigoni, M. Macagno, S. Pizzimenti, L. Aurisicchio, F. Cavallo
Analysis and interpretation of data (e.g., statistical analysis, biostatistics, computational analysis): S. Lanzardo, L. Conti, R. Rooke, R. Ruiu, N. Accart, M. Arigoni, M. Macagno, R.A. Calogero, F. Cavallo
Writing, review, and/or revision of the manuscript: S. Lanzardo, L. Conti, R. Rooke, R. Ruiu, N. Accart, M. Arigoni, M. Macagno, G. Barrera, F. Cavallo
Administrative, technical, or material support (i.e., reporting or organizing data, constructing databases): F. Cavallo
Study supervision: F. Cavallo

Grant Support

This work has been supported with grants from the Italian Association for Cancer Research (IG 11675), Fondazione Ricerca Molinette Onlus, the University of Turin, and the Compagnia di San Paolo (Progetti di Ricerca Ateneo/CSP). L. Conti has been supported with a fellowships from the Fondazione Umberto Veronesi, "Pink is Good" project.

The costs of publication of this article were defrayed in part by the payment of page charges. This article must therefore be hereby marked *advertisement* in accordance with 18 U.S.C. Section 1734 solely to indicate this fact.

Received May 11, 2015; revised September 9, 2015; accepted September 30, 2015; published OnlineFirst November 13, 2015.

References

1. Siegel R, DeSantis C, Virgo K, Stein K, Mariotto A, Smith T, et al. Cancer treatment and survivorship statistics, 2012. *CA Cancer J Clin* 2012;62:220-41.
2. Frank NY, Schatton T, Frank MH. The therapeutic promise of the cancer stem cell concept. *J Clin Invest* 2010;120:41-50.
3. Ning N, Pan Q, Zheng F, Teitz-Tennenbaum S, Egenti M, Yet J, et al. Cancer stem cell vaccination confers significant antitumor immunity. *Cancer Res* 2012;72:1853-64.
4. Kwiatkowska-Borowczyk EP, Gabka-Buszek A, Jankowski J, Mackiewicz A. Immunotargeting of cancer stem cells. *Contemp Oncol* 2015;19:A52-9.
5. Aurisicchio L, Ciliberto G. Genetic cancer vaccines: current status and perspectives. *Expert Opin Biol Ther* 2012;12:1043-58.
6. Rovero S, Amici A, Di Carlo E, Bei R, Nanni P, Quaglino E, et al. DNA vaccination against rat her-2/Neu p185 more effectively inhibits carcinogenesis than transplantable carcinomas in transgenic BALB/c mice. *J Immunol* 2000;165:5133-42.
7. Lewerenz J, Hewett SJ, Huang Y, Lambros M, Gout PW, Kalivas PW, et al. The cystine/glutamate antiporter system x(c)(-) in health and disease: from molecular mechanisms to novel therapeutic opportunities. *Antioxid Redox Signal* 2013;18:522-55.

8. Gout PW, Buckley AR, Simms CR, Bruchovsky N. Sulfasalazine, a potent suppressor of lymphoma growth by inhibition of the x(c)-cystine transporter: a new action for an old drug. *Leukemia* 2001;15:1633–40.
9. Chung WJ, Lyons SA, Nelson GM, Hamza H, Gladson CL, Gillespie GY, et al. Inhibition of cystine uptake disrupts the growth of primary brain tumors. *J Neurosci* 2005;25:7101–10.
10. Narang VS, Pauletti GM, Gout PW, Buckley DJ, Buckley AR. Suppression of cystine uptake by sulfasalazine inhibits proliferation of human mammary carcinoma cells. *Anticancer Res* 2003;23:4571–9.
11. Doxsee DW, Gout PW, Kurita T, Lo M, Buckley AR, Wang Y, et al. Sulfasalazine-induced cystine starvation: potential use for prostate cancer therapy. *Prostate* 2007;67:162–71.
12. Jiang L, Kon N, Li T, Wang SJ, Su T, Hibshoosh H, et al. Ferroptosis as a p53-mediated activity during tumour suppression. *Nature* 2015;520:57–62.
13. Ishimoto T, Nagano O, Yae T, Tamada M, Motohara T, Oshima H, et al. CD44 variant regulates redox status in cancer cells by stabilizing the xCT subunit of system xc(-) and thereby promotes tumor growth. *Cancer Cell* 2011;19:387–400.
14. Timmerman LA, Holton T, Yuneva M, Louie RJ, Padro M, Daemen A, et al. Glutamine sensitivity analysis identifies the xCT antiporter as a common triple-negative breast tumor therapeutic target. *Cancer Cell* 2013;24:450–65.
15. Chen RS, Song YM, Zhou ZY, Tong T, Li Y, Fu M, et al. Disruption of xCT inhibits cancer cell metastasis via the caveolin-1/beta-catenin pathway. *Oncogene* 2009;28:599–609.
16. Huang Y, Dai Z, Barbacioru C, Sadee W. Cystine-glutamate transporter SLC7A11 in cancer chemosensitivity and chemoresistance. *Cancer Res* 2005;65:7446–54.
17. Yoshikawa M, Tsuchihashi K, Ishimoto T, Yae T, Motohara T, Sugihara E, et al. xCT inhibition depletes CD44v-expressing tumor cells that are resistant to EGFR-targeted therapy in head and neck squamous cell carcinoma. *Cancer Res* 2013;73:1855–66.
18. Conti L, Lanzardo S, Arigoni M, Antonazzo R, Radaelli E, Cantarella D, et al. The noninflammatory role of high mobility group box 1/Toll-like receptor 2 axis in the self-renewal of mammary cancer stem cells. *FASEB J* 2013;27:4731–44.
19. Quaglino E, Mastini C, Amici A, Marchini C, Iezzi M, Lanzardo S, et al. A better immune reaction to ErbB-2 tumors is elicited in mice by DNA vaccines encoding rat/human chimeric proteins. *Cancer Res* 2010;70:2604–12.
20. Donato MT, Martinez-Romero A, Jimenez N, Negro A, Herrera G, Castell JV, et al. Cytometric analysis for drug-induced steatosis in HepG2 cells. *Chem Biol Interact* 2009;181:417–23.
21. Fend L, Accart N, Kintz J, Cochin S, Reymann C, Le Pogam F, et al. Therapeutic effects of anti-CD115 monoclonal antibody in mouse cancer models through dual inhibition of tumor-associated macrophages and osteoclasts. *PLoS One* 2013;8:e73310.
22. Ravindranath V. Animal models and molecular markers for cerebral ischemia-reperfusion injury in brain. *Methods Enzymol* 1994;233:610–9.
23. Sedlak J, Lindsay RH. Estimation of total, protein-bound, and nonprotein sulfhydryl groups in tissue with Ellman's reagent. *Anal Biochem* 1968;25:192–205.
24. Nanni P, Landuzzi L, Nicoletti G, De Giovanni C, Rossi I, Croci S, et al. Immunoprevention of mammary carcinoma in HER-2/neu transgenic mice is IFN-gamma and B cell dependent. *J Immunol* 2004;173:2288–96.
25. Arigoni M, Barutello G, Lanzardo S, Longo D, Aime S, Curcio C, et al. A vaccine targeting angiominin induces an antibody response which alters tumor vessel permeability and hampers the growth of established tumors. *Angiogenesis* 2012;15:305–16.
26. Grange C, Lanzardo S, Cavallo F, Camussi G, Bussolati B. Sca-1 identifies the tumor-initiating cells in mammary tumors of BALB-neuT transgenic mice. *Neoplasia* 2008;10:1433–43.
27. Riccardo F, Arigoni M, Buson G, Zago E, Iezzi M, Longo D, et al. Characterization of a genetic mouse model of lung cancer: a promise to identify non-small cell lung cancer therapeutic targets and biomarkers. *BMC Genomics* 2014;15 Suppl 3:S1.
28. Lo M, Wang YZ, Gout PW. The x(c)-cystine/glutamate antiporter: a potential target for therapy of cancer and other diseases. *J Cell Physiol* 2008;215:593–602.
29. Sithanandam G, Anderson LM. The ERBB3 receptor in cancer and cancer gene therapy. *Cancer Gene Ther* 2008;15:413–48.
30. Schwitalla S. Tumor cell plasticity: the challenge to catch a moving target. *J Gastroenterol* 2014;49:618–27.
31. Kinoshita H, Okabe H, Beppu T, Chikamoto A, Hayashi H, Imai K, et al. Cystine/glutamic acid transporter is a novel marker for predicting poor survival in patients with hepatocellular carcinoma. *Oncol Rep* 2013;29:685–9.
32. Sugano K, Maeda K, Ohtani H, Nagahara H, Shibutani M, Hirakawa K. Expression of xCT as a predictor of disease recurrence in patients with colorectal cancer. *Anticancer Res* 2015;35:677–82.
33. Singer E, Judkins J, Salomonis N, Matlaf L, Soteropoulos P, McAllister S, et al. Reactive oxygen species-mediated therapeutic response and resistance in glioblastoma. *Cell Death Dis* 2015;6:e1601.
34. Sato A, Okada M, Shibuya K, Watanabe E, Seino S, Narita Y, et al. Pivotal role for ROS activation of p38 MAPK in the control of differentiation and tumor-initiating capacity of glioma-initiating cells. *Stem Cell Res* 2014;12:119–31.
35. Shi X, Zhang Y, Zheng J, Pan J. Reactive oxygen species in cancer stem cells. *Antioxid Redox Signal* 2012;16:1215–28.
36. Ryoo IG, Choi BH, Kwak MK. Activation of NRF2 by p62 and proteasome reduction in sphere-forming breast carcinoma cells. *Oncotarget* 2015;6:8167–84.
37. Mizuno T, Suzuki N, Makino H, Furui T, Morii E, Aoki H, et al. Cancer stem-like cells of ovarian clear cell carcinoma are enriched in the ALDH-high population associated with an accelerated scavenging system in reactive oxygen species. *Gynecol Oncol* 2015;137:299–305.
38. Linares V, Alonso V, Domingo JL. Oxidative stress as a mechanism underlying sulfasalazine-induced toxicity. *Expert Opin Drug Saf* 2011;10:253–63.
39. de la Fuente V, Federman N, Fustinana MS, Zalman G, Romano A. Calcineurin phosphatase as a negative regulator of fear memory in hippocampus: control on nuclear factor-kappaB signaling in consolidation and reconsolidation. *Hippocampus* 2014;24:1549–61.
40. Dai L, Cao Y, Chen Y, Parsons C, Qin Z. Targeting xCT, a cystine-glutamate transporter induces apoptosis and tumor regression for KSHV/HIV-associated lymphoma. *J Hematol Oncol* 2014;7:30.
41. Robe PA, Martin DH, Nguyen-Khac MT, Artesi M, Deprez M, Albert A, et al. Early termination of ISRCTN45828668, a phase 1/2 prospective, randomized study of sulfasalazine for the treatment of progressing malignant gliomas in adults. *BMC Cancer* 2009;9:372.
42. Aurisicchio L, Mancini R, Ciliberto G. Cancer vaccination by electro-gene-transfer. *Expert Rev Vaccines* 2013;12:1127–37.
43. Rolla S, Nicolo C, Malinarich S, Orsini M, Forni G, Cavallo F, et al. Distinct and non-overlapping T cell receptor repertoires expanded by DNA vaccination in wild-type and HER-2 transgenic BALB/c mice. *J Immunol* 2006;177:7626–33.
44. Liao WT, Ye YP, Deng YJ, Bian XW, Ding YQ. Metastatic cancer stem cells: from the concept to therapeutics. *Am J Stem Cells* 2014;3:46–62.
45. Partridge WM. The blood-brain barrier: bottleneck in brain drug development. *NeuroRx* 2005;2:3–14.
46. Srivastava MK, Sinha P, Clements VK, Rodriguez P, Ostrand-Rosenberg S. Myeloid-derived suppressor cells inhibit T-cell activation by depleting cystine and cysteine. *Cancer Res* 2010;70:68–77.
47. McCullagh EA, Featherstone DE. Behavioral characterization of system xc- mutant mice. *Behav Brain Res* 2014;265:1–11.
48. Conklin KA. Chemotherapy-associated oxidative stress: impact on chemotherapeutic effectiveness. *Integr Cancer Ther* 2004;3:294–300.
49. Narang VS, Pauletti GM, Gout PW, Buckley DJ, Buckley AR. Sulfasalazine-induced reduction of glutathione levels in breast cancer cells: enhancement of growth-inhibitory activity of Doxorubicin. *Chemotherapy* 2007;53:210–7.
50. Wang F, Yang Y. Suppression of the xCT-CD44v antiporter system sensitizes triple-negative breast cancer cells to doxorubicin. *Breast Cancer Res Treat* 2014;147:203–10.